Operational Assimilation of Space-Borne Radar and Lidar Cloud Profile Observations for Numerical Weather Prediction

ESA-ESTEC Contract Nr. 4000116891/16/NL/LvH

EXECUTIVE SUMMARY REPORT

Authors: Marta Janisková and Mark Fielding

European Centre for Medium-Range Weather Forecasts
Reading, UK

September 2018

Operational Assimilation of Space-borne Radar and Lidar Cloud Profile Observations for Numerical Weather Prediction

ESA-ESTEC Contract Nr. **4000116891/16/NL/LvH**

Executive Summary Report

Issue: 1.0
September 2018

Written: Marta Janisková and Mark Fielding

Approved:

Authorised:

This page intentionally left blank

Summary Report for the project Operational Assimilation of Space-borne Radar and Lidar Cloud Profile Observations for Numerical Weather Prediction

M. Janisková and M. Fielding

ECMWF, Reading, U.K.

1 Introduction

Cloud radar and lidar measurements contain a wealth of information on the vertical structure of clouds and precipitation. However, the only cloud-affected observations routinely assimilated in global numerical weather prediction (NWP) models are microwave radiance observations, which contain limited information on cloud structure. Observations providing vertical information on clouds from space-borne active instruments on board of CloudSat (Stephens et al., 2002) and CALIPSO (Cloud-Aerosol Lidar and Infrared Pathfinder Satellite Observations, Winker et al., 2009) are already available and new ones, such as Earth, Clouds, Aerosols and Radiation Explorer (EarthCARE, Illingworth et al., 2015) should appear in the near future. The EarthCARE mission (ESA, 2004) will provide the vertically resolved characterization of clouds by the combination of lidar (Atmospheric Lidar, ATLID) and a cloud profiling radar (CPR).

A number of studies, including the European Space Agency (ESA) funded project Quantitative Assessment of the Operational Value of Space-Borne Radar and Lidar Measurements of Cloud and Aerosol Profiles (QuARL, Janisková et al., 2010), have shown that observations of clouds from space-borne radar and lidar are useful not only to evaluate the performance of current NWP models in representing clouds, precipitation and aerosols, but they have also the potential to be assimilated into these models to improve their initial atmospheric state. The subsequent study (STSE Study - EarthCARE Assimilation, Janisková et al., 2014) focused on the development of an off-line system to monitor/assimilate space-borne radar and lidar observations in clouds within the NWP model of the European Centre for Medium-Range Weather Forecasts (ECMWF) in order to prepare for the exploitation of radar and lidar observations in data assimilation. The studies using a technique combining one-dimensional variational (1D-Var) assimilation with four-dimensional variational (4D-Var) data assimilation provided indications on the potential that assimilation of cloud information from active sensors could offer.

Inspired by the success of 1D+4D-Var experiments, the current project has focused on developments towards direct assimilation and monitoring systems to exploit cloud radar and lidar data for their assimilation in NWP models. The direct (in-line) data assimilation and monitoring systems developed during this project allow extended research studies beneficial for future applications of EarthCARE ATLID and CPR data once available on the global scale.

2 Observation processing

2.1 Observation operator developments and updates

The observation operator is a fundamental part of data assimilation as it transforms model variables to observations, thus allowing the model fit to observations to be assessed and improved. The observation operators for radar reflectivity and lidar backscatter within the Integrated Forecasting System (IFS) model were developed in two previous projects (QuARL, Janisková et al., 2010; and STSE Study - EarthCARE Assimilation, Janisková et al., 2014), however in this current project they have been updated for in-line assimilation, where operational constraints require a balance of efficiency and complexity. There has also been a focus on consistency; the assumptions made in the observation operators have been modified to be consistent with each other, and (as much as possible) consistent with other forward models and parameterizations in the ECMWF 4D-Var assimilation and forecasting systems. Without consistency, observation operators for different observation types could work against each other, preventing the model initial state from getting closer to the truth.

Two major updates were made to the operator to improve efficiency. The first was to introduce a parameterization of the hydrometeor scattering properties. In the original version of the operator, the scattering properties were found using a pre-computed look-up table as a function of temperature and in-cloud water content. Through experimentation it was found that both radar reflectivity and lidar backscatter could be approximated by a two-variable two-degree polynomial with six fitting coefficients. Secondly a much more efficient way to handle cloud overlap was devised. By partitioning the transmission into a cloudy and a clear column, similar results can now be obtained as from the original multi-column method, which requires the computation of at least 20 sub-columns and is not differentiable and therefore was used for monitoring and evaluation only. The development of the double-column method allows cloud overlap to be specified in the data assimilation, which should improve the assimilation of lidar in scenes with strong attenuation, such as multi-layer clouds.

Considering all the updates to the observation operator for radar reflectivity, Fig. 1 shows the frequency distribution of radar reflectivity with temperature for CloudSat observations, the previous version of the observation operator and the latest version of the operator. In particular, this figure highlights the new particle size distribution chosen for stratiform rain Abel and Boutle (2012). The new scheme's shift towards smaller drops for smaller water contents results in a significant reduction in radar reflectivity for water content less than 0.01 g m^{-3}, providing a much better fit to observations. Other modifications to the microphysical assumptions of the operator were designed to match those in the IFS cloud scheme and with each other, such as changing the ice cloud particle habit.

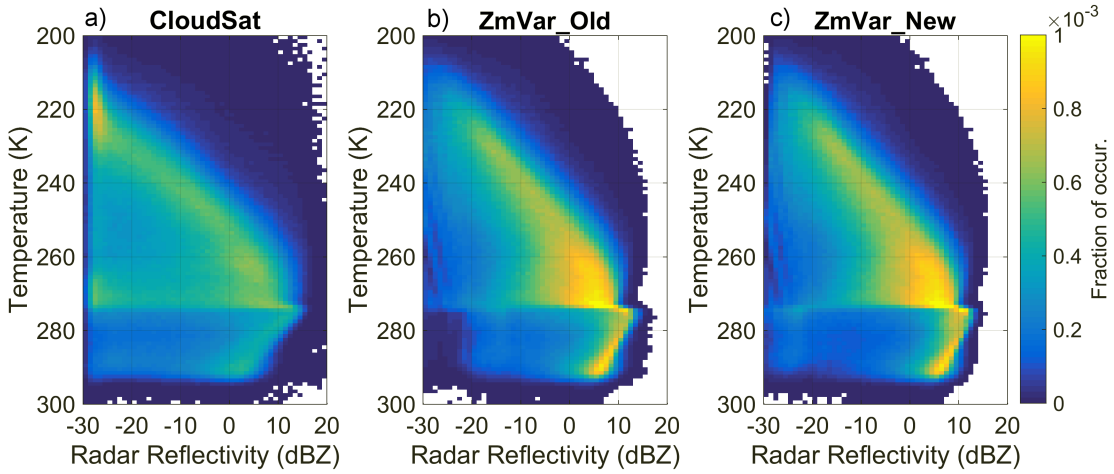

Figure 1: *Frequency distribution of observed and simulated radar reflectivity with temperature. Panel (a) shows CloudSat observations for August 2007 after averaging at model resolution. Panels (b) and (c) show the simulated reflectivity using the original and updated lookup tables, respectively.*

2.2 Observation pre-processing

To enable the in-line assimilation of radar reflectivity and lidar backscatter within the ECMWF 4D-Var assimilation system significant developments, both scientific and technical, were required. Firstly the quality control and bias correction schemes needed to be refined and compared to those used in the 1D+4D-Var experiments.

2.2.1 Quality control and screening

Quality control and screening help to prevent observations that will have a negative impact on the data assimilation analysis and subsequent forecast from entering the system. There are several reasons that an observation may not have a positive impact; they may be unphysical, the forward model may not be capable of representing the observation, or they may cause excessive non-linearities in the observation operator. New screening indicators included the blacklisting of excessively attenuated signals in the lidar backscatter, situations with radar multiple scattering and model levels with small cloud fraction.

2.2.2 Bias correction

Due to the updates in the observation operators and the new screening criteria, a new bias correction scheme was required. A bias correction scheme is an important component of any data assimilation system as it ensures systematic biases, which can have a detrimental impact on the analysis, are removed. The bias correction scheme is based on indicators of height and temperature, thus providing an implicit regime dependence. Joint probability density plots of simulated and observed radar reflectivity before and after the bias correction has been applied are shown in Fig. 2.

For the radar reflectivity, in a global sense, the difference between observations and model equivalent is remarkably unbiased and a strong correlation (a correlation coefficient of approximately 0.7) is apparent. After bias correction, the slight underestimation of precipitation was corrected and the overestimation of ice cloud reflectivity was reduced. For the lidar backscatter, the difference between observations and model equivalent are greater and the correlation is less than seen for the radar reflectivity. An underestimation in the ice cloud (with first guess around -30 dBβ) was corrected by applying bias correction.

The bias correction will need to be recomputed each time either the IFS model or the observation operator is updated as both will affect any systematic biases present. However, as the framework has been constructed, it should be straight-forward to generate, providing the changes do not warrant the selection of different indicators. In an operational context, it would be desirable to use variational bias correction where biases are automatically corrected within 4D-Var, but this would require at least six months of stable observations and significant efforts to ensure the system was performing correctly.

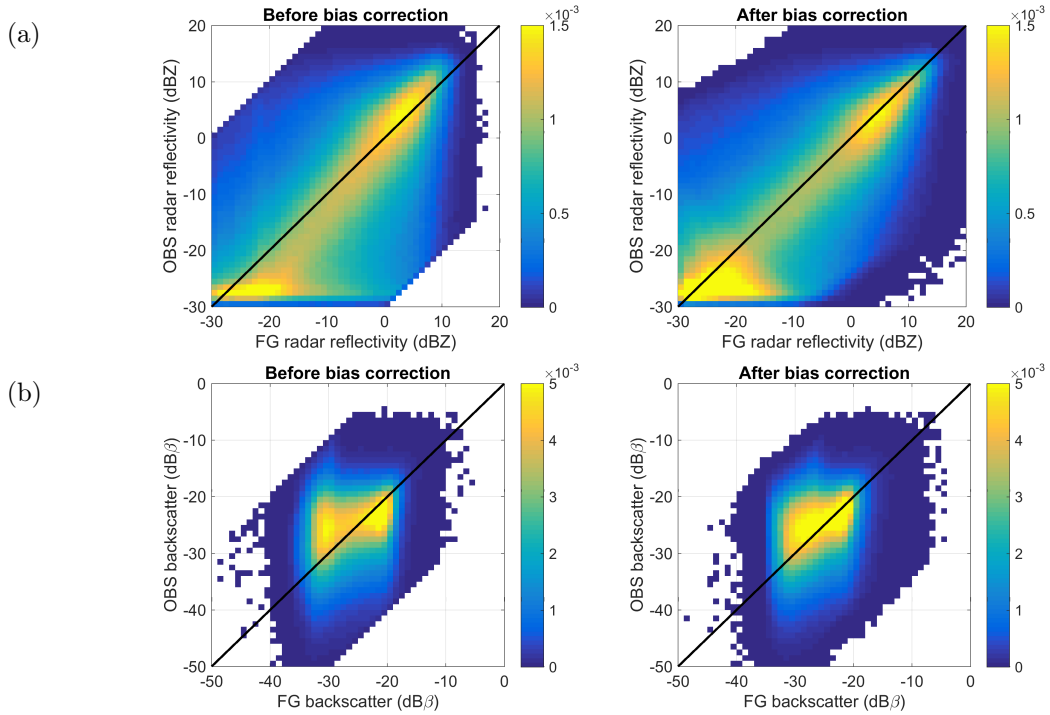

Figure 2: *Joint probability density plots of (a) simulated radar reflectivity and observed CloudSat radar reflectivity, and (b) simulated lidar backscatter and CALIPSO lidar attenuated backscatter using observations during September 2007. The left panel shows data before bias correction, while the right panel shows the relationship after bias correction. Only data passing quality control are considered.*

2.2.3 Observation error

To combine the observations and the model, the data assimilation system requires an estimate of the observation error. Following the approach taken in previous projects, we assume that the observation error is a function of measurement error, representativity error and forward model error. By computing these constituent parts, a physically based estimate of the observation error is obtained. To model the representativity error, a new technique is implemented that uses the local variability along the transect combined with the climatological correlation. The new method has been validated using synthetic data and MODIS radiances and has similar performance to a more complex method based on look-up tables

(Stiller, 2010). To obtain estimates of forward model error, we use a Monte Carlo approach (similar to, e.g., Kulie et al., 2010; Di Michele et al., 2012), where microphysical assumptions are perturbed within their physical ranges. With all components combined, this physically based estimate of observation error has the advantage of being independent from the model background errors and should give a better estimate of the true observation error, thus optimising the observation's use.

Figure 3 shows the mean observation error calculated for one month of CloudSat and CALIPSO observations. For CloudSat radar reflectivity, representativity error tends to dominate over tropical areas, while forward model error dominates the extra-tropics, particularly in stratiform regimes. Conversely, for CALIPSO lidar backscatter, the observation error tends to be less in the tropics as the lidar has the smallest errors for regions associated with ice cloud, such as those formed by convective outflow. The spatial magnitude of observation error for both CloudSat and CALIPSO also compares favourably with the standard deviation of first guess departures.

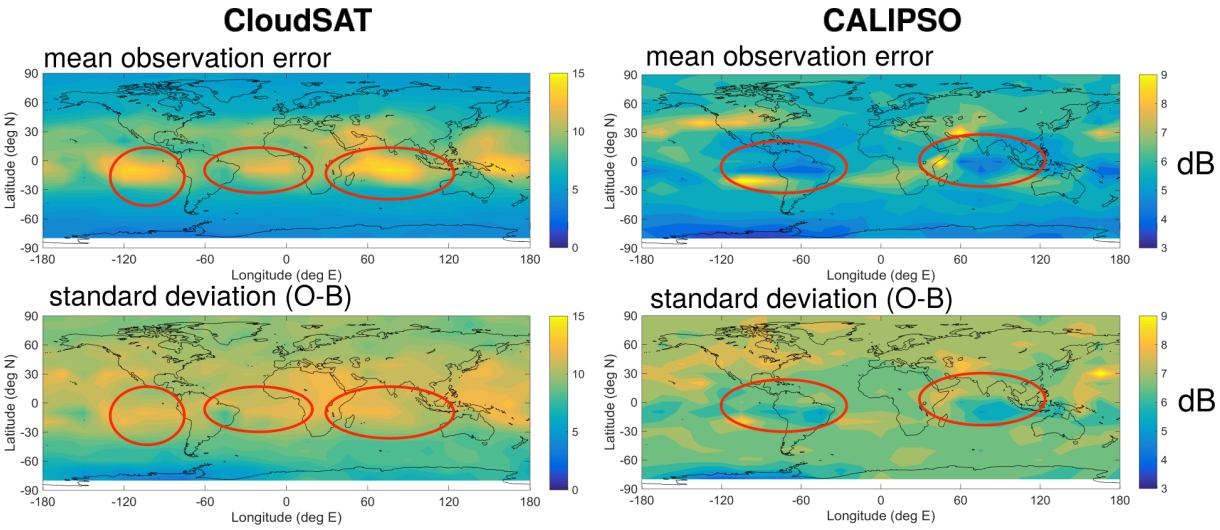

Figure 3: *A comparison of global maps of CloudSat radar (left side) and CALIPSO lidar (right side) mean expected observation errors (sum of instrument, operator and representativity errors; top) versus the standard deviation of first guess departure errors (bottom). The red ovals are to aid comparison.*

2.3 Adjustments required for the EarthCARE observations

The CloudSat radar and CALIOP (Cloud-Aerosol Lidar with Orthogonal Polarization) lidar share many characteristics of the EarthCARE CPR and ATLID and have been considered synonymous for technical testing and feasibility studies. However, to assimilate the CPR and the ATLID with scientific meaning, several modifications were required. For the radars, the main differences between the instruments relate to the larger antenna of the CPR, which leads to greater sensitivity and reduced multiple scattering. The CPR also detects the phase shift of signals, such that the Doppler velocity of targets can be measured. For the lidars, the differences are potentially more significant; the wavelength of the instruments are also different, which leads to different cloud and molecular scattering properties. The smaller field of view of the ATLID also leads to reduced multiple scattering.

The main conclusions from adapting the forward models to EarthCARE specifications were firstly that the CPR will detect significantly smaller hydrometeors (the 7 dB increase in sensitivity will detect particles with up to 30% smaller radii), which should halve the number of clouds missed (particularly ice clouds) and allow greater synergy with the lidar. Secondly, the sensitivity in total attenuated backscatter is less for ATLID due to the increased molecular backscatter at 355nm compared to CALIPSO. Finally, the effects of multiple scattering are likely be similar in the two lidars due to compensating effects of ATLID's narrower field of view, yet shorter wavelength.

Technical changes needed to process the EarthCARE data into a format that can be ingested and used by the data assimilation system were also developed. Changes to the data selection, pre-processing and screening were needed, particularly in relation to the cloud masks, which will not be provided in the L1b raw data. Tests demonstrating the technical capability of the system to assimilate EarthCARE data were made, making use of the A-NOM and C-NOM test data produced using a high-resolution model and the EarthCARE Simulator.

3 Data monitoring of cloud radar and lidar observations

Before any new observations are actively assimilated in the ECMWF 4D-Var system, they are passively monitored, along with all assimilated observations, ensuring both the observations and model are behaving as expected. Due to the vast quantities of data involved, the monitoring system at ECWMF is automated, where selected indicators are checked against expected ranges. Alerts are automatically triggered and sent to analysts for further investigation if the observations exceed these ranges. In addition, alerts can be sent to other relevant parties, including instrument mentors, which could be critical in detecting and correcting problems with satellite data in a timely manner.

To set up the automated monitoring system for cloud radar and lidar data, indicators were chosen and statistics generated to set the expected ranges of the data. Figure 4 shows statistics for 12-hour mean indicators of observation value only and the first guess departures for both radar reflectivity and lidar backscatter. The hard limits, designed to detect drifts in the observations or model are set (red dashed lines) using a threshold in the standard deviation. As the indicators' distributions resemble normal distributions, the data is suitable for monitoring and detecting errors.

To show the power of combining observations and model information within a monitoring system, an experiment was carried out where artificial drifts were applied to CloudSat and CALIPSO data. Figure 5 shows an example where a 1% decrease per day was applied to the CloudSat radar reflectivity,

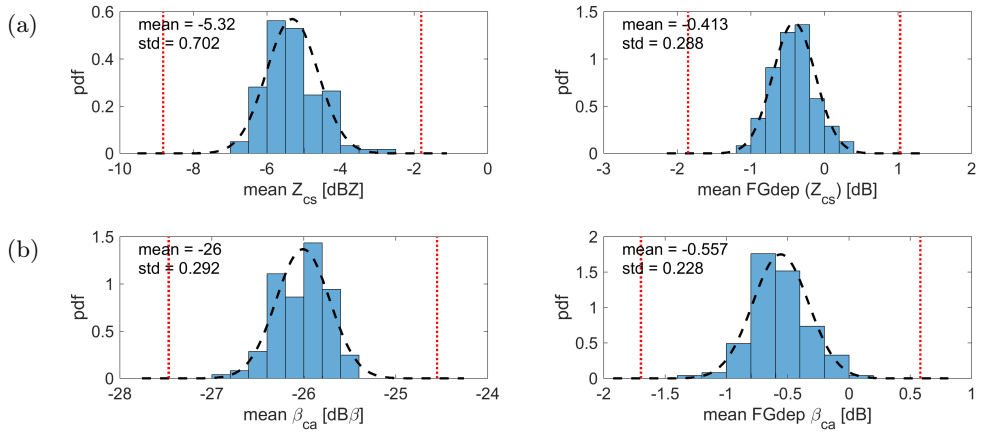

Figure 4: *Histograms of 12-hour global mean observations and their model equivalent between August - September 2007. Panels on left side show observations: (a) CloudSat radar reflectivity and (b) CALIPSO lidar attenuated backscatter. Panels on right side show corresponding observation and model equivalent - mean FG departures. The black dashed lines show the Gaussian distribution with the mean and standard deviation of the data. The red dotted lines indicate 5 standard deviations from the mean.*

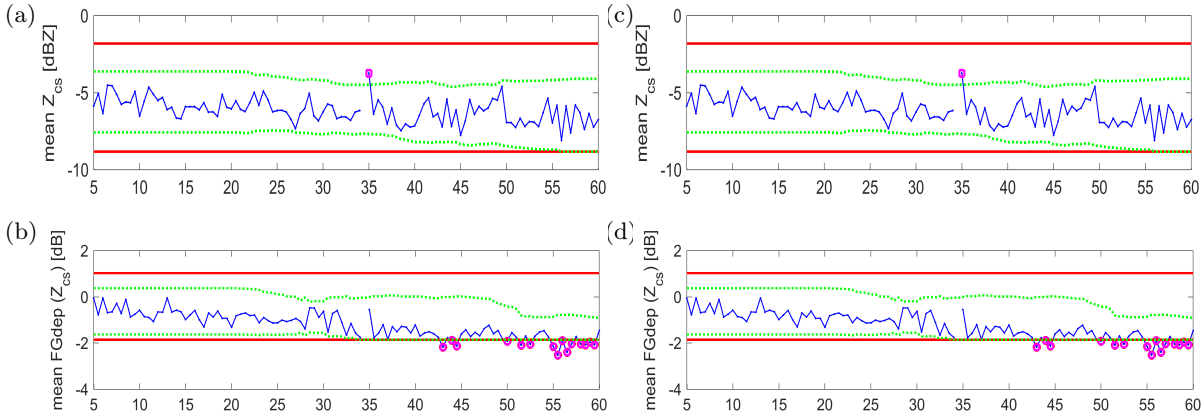

Figure 5: *Example of CloudSat (left) and CALIPSO (right) data within the automatic monitoring system using observation-only indicators of global mean (a) radar reflectivity or (c) lidar attenuated backscatter and using combined observation and model indicators of global mean first guess departures where a 1% per day drift in observed (b) radar reflectivity or (d) attenuated lidar backscatter has been introduced at day 10.*

leading to a total bias of 3 dB after two months. No automatic alerts due to the drift were triggered when considering observations only (Fig. 5a), whereas alerts were triggered around 30 days after the bias was introduced when considering the combination of observations and model (Fig. 5b). A similar conclusion was reached when considering the artificial drift in CALIPSO observations of lidar backscatter (Fig. 5 c,d).

4 Data assimilation experiments for radar and lidar

4.1 Performed experiments

In order to study the impact of new space-borne cloud radar and lidar observations on analyses and subsequent forecasts, the 4D-Var assimilation system used at ECMWF needed to be updated. This required a lot of technical development, such as implementing the modifications and developments to observation operators, observation error definition and data handling for observations (i.e. quality control, screening and bias correction) as described in the previous sections. After technical testing of the correctness of the updated system, 4D-Var assimilation experiments have been performed using CloudSat cloud radar reflectivity and CALIPSO lidar backscatter. Using the full system of regularly assimilated observations at ECMWF and assimilation cycles of 12-hours (i.e. the current length of 4D-Var assimilation window at ECMWF), several experiments have been performed over 10 days covering 1-10 August 2007 period adding the new observations to the system. 4D-Var experimentation has been done using a horizontal resolution of TCo639 spectral truncation (corresponding to approximately 18 km on a cubic octahedral grid) and 137 vertical levels.

Several 4D-Var experiments have been run with different setups to study the impact of the new cloud radar and lidar observations, either each of them separately or together and then without or in combination with other regularly assimilated observations. The impact of observation error definition on the performance has been also investigated. From obtained 4D-Var analyses, 10 day forecasts have been run to study the impact of these new observations on the subsequent forecasts.

4.2 Summary of the results

4.2.1 Impact on the analysis

The performed experiments have shown that 4D-Var provides analysis departures closer to cloud radar and lidar observations than would be obtained if these observations were not assimilated. Probability distribution function (PDF) of the first-guess (FG) and analysis (AN) departures for the cloud radar reflectivity and lidar backscatter shown on Fig. 6 for the different assimilation experiments (as specified in figure caption) indicates that analysis including radar and lidar observations together with all other normally assimilated observations provides better PDF distribution than the reference run. Obviously, the most symmetric PDF shapes are achieved when assimilating just the new observations alone.

The fact that the analysis is drawn to the radar and lidar observations has been also demonstrated by an along-track evaluation (Fig. 7 - 8) where the impact of individual clouds can be assessed. As expected, the analysis provides a closer fit to the observations which is more pronounced for the analysed radar reflectivity (Fig. 7c). The model is not drawn as strongly to cloud lidar backscatter observations (Fig. 8c) perhaps due to ambiguities in generating the analysis increments; increasing cloud amount at the top of the cloud to match the observations could also result in corrections of the departures at the base of the cloud due to the increased attenuation of the modelled signal leading to an excess of cloud in the model. Investigations will be done whether assimilating the whole profile rather than just when there is cloud in both model and observations might help to solve this problem. But overall, impact of the new observations on 4D-Var analysis when compared against own observations based on statistics for 10 days of assimilating cycling further confirmed that analysis is getting closer to these observations.

Verification of the performed assimilation runs has also been carried out against other assimilated observation types in 4D-Var. The results indicated that mainly for conventional observations (such as TEMP radiosonde, PILOT or AIREP observations), bias and standard deviations of the background departures are overall marginally smaller in the experimental runs compared to the reference run not using the new cloud radar and lidar observations (Fig. 9). The largest impact of these observations is observed for wind. For all other types of observations assimilated in 4D-Var, no significant changes

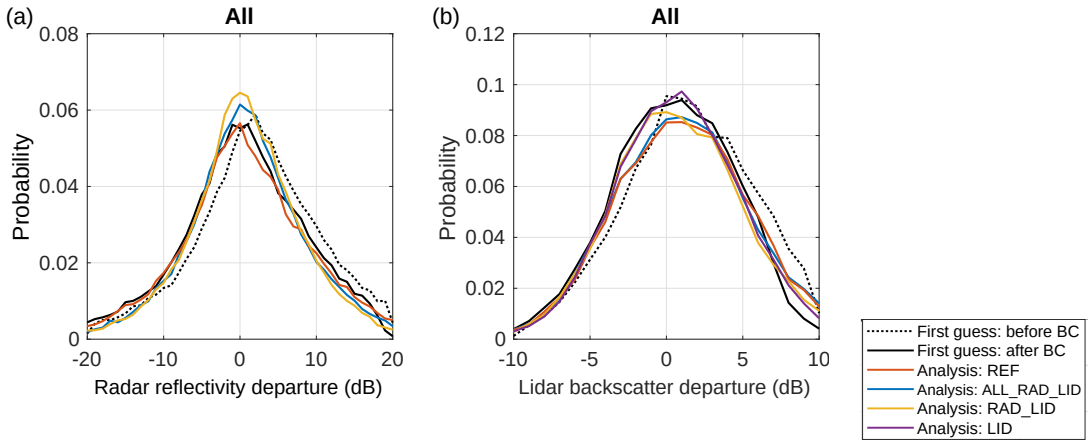

Figure 6: *Probability distribution functions of the first guess departures before (black dotted line) and after (black solid line) bias correction applied combined with the analysis departures for the reference experiment (***REF***, red solid line), experiment assimilating cloud radar and lidar observations with all other normally assimilated observations (***ALL_RAD_LID***, blue solid line), experiment assimilating cloud radar and lidar observations only (***RAD_LID***, orange solid line) and assimilation using lidar observations only (***LID***, violet solid line). Results are presented for (a) radar reflectivity and (b) lidar backscatter departures (dB) over the whole globe. Situation* **2007080100** *with 12-hour assimilation period between 31 July 2007 21:00 UTC and 1 August 2007 09:00 UTC.*

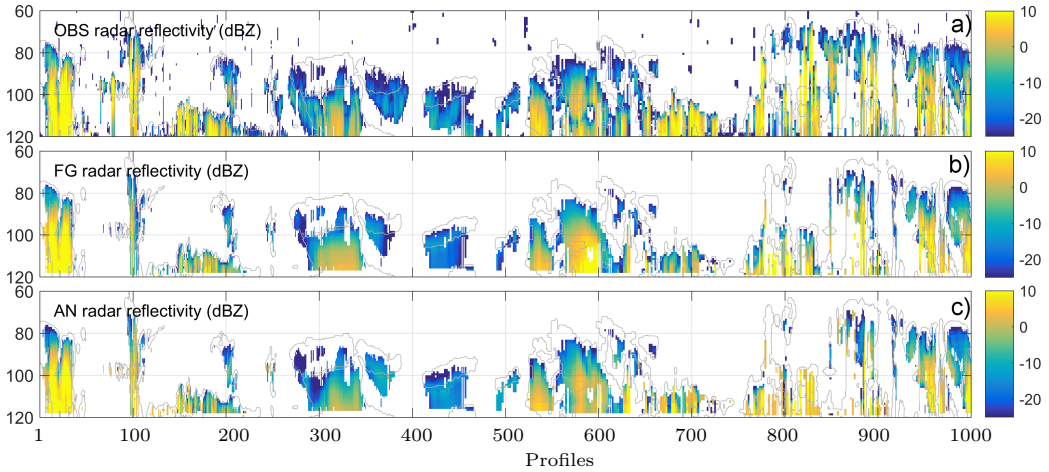

Figure 7: *Cross-sections of radar reflectivity related variables corresponding to the portion of orbital track (21:00 UTC 31st July 2007). Panels show (a) observed CloudSat radar reflectivity (dBZ), (b) model equivalent (FG) radar reflectivity using the model background (dBZ) and (c) model equivalent (AN) radar reflectivity using the model analysis from the assimilation experiment using all observations with radar and lidar (***ALL_RAD_LID***). Note that the first guess radar reflectivity is only displayed where there are hydrometeors detected in both model and observations. To elucidate the position of the model clouds, the first-guess model cloud boundaries are shown in grey.*

have appeared when considering FG and AN departure statistics. Generally, it is not easy to achieve a significant improvement in the experimental run compared to the reference one over a domain well covered by a large amount of other measurements. Therefore any improvement is encouraging since it indicates a potential benefit from assimilating cloud information.

4.2.2 Impact on the subsequent forecast

Assimilating cloud radar and lidar was shown to reduce forecast errors, particularly in temperature and wind. The evaluation of the impact of the assimilation of cloud radar and lidar observations on the skill of subsequent forecasts has been done in terms of differences in the root-mean-square (RMS) forecast error between the forecasts starting from analysis assimilating these new observations

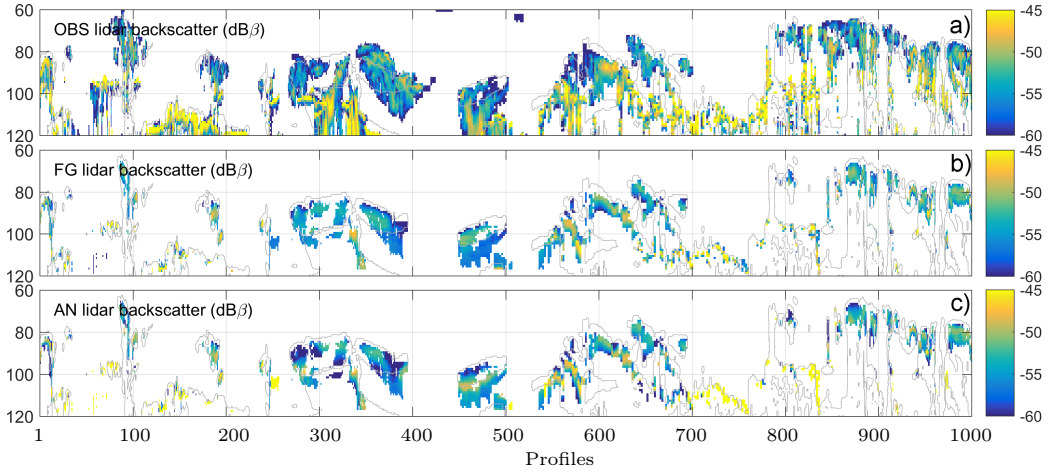

Figure 8: *Same as Fig. 7, but for CALIPSO lidar backscatter.*

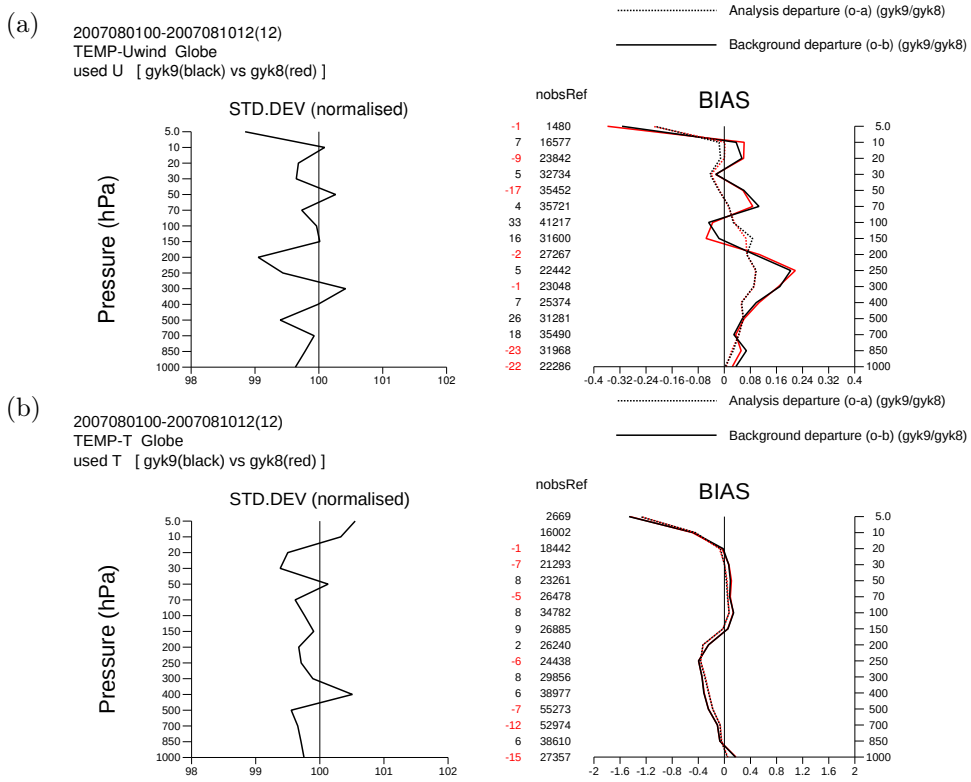

Figure 9: *Normalised standard deviation (left) and bias (right) of background (solid line) and analysis departures (dotted line) with respect to TEMP (a) zonal wind and (b) temperature observations for the reference run (***REF***, red) and experiment assimilating in addition cloud radar reflectivity and lidar backscatter observations (***ALL_RAD_LID***, black) using double observation errors. The number of observations for* **REF** *experiment (nobsRef) for the period 1 August 2007 00:00 UTC - 10 August 2007 12:00 UTC is displayed in the middle together with negative red and positive black numbers indicating how many less or more, respectively, observations are used by the* **ALL_RAD_LID** *run. Results are shown for the whole globe.*

and the forecast starting from the reference analysis. Both experiment's forecast errors have been computed with respect to the operational analysis. Zonal means of these RMS error differences are shown for temperature and zonal wind in Fig. 10 for one assimilation cycle with the analysis time 00:00 UTC 1 August 2007. The forecast generated using the experimental analysis shows an increase in forecast skill of temperature and wind, with the greatest increases in three regions; one in the Northern Hemisphere extra-tropics, one just north of the equator corresponding to the Inter-Tropical

Convergence Zone (ITCZ), and a third in the Southern Hemisphere extra-tropics. These three regions correspond to locations with the greatest quantity of cloud and hence radar and lidar observations.

Investigation of the forecast skill by verification of the forecast against operational analyses also indicated that while the radar provided the largest impact on forecast errors, assimilating both radar and lidar has the greatest total benefit to the forecast.

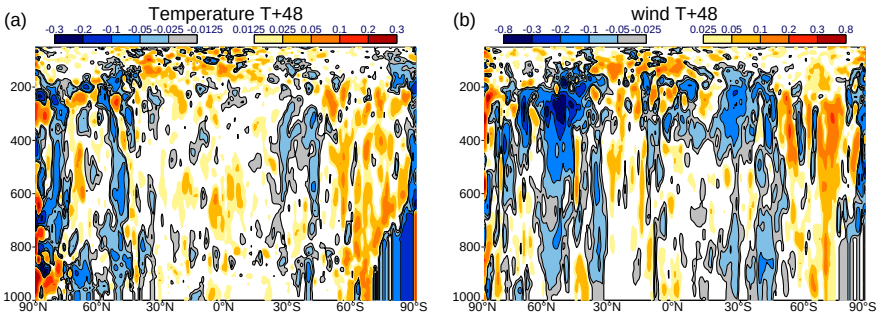

Figure 10: *Zonal mean of differences of (a) temperature (K) and (b) wind (m s^{-1}) RMS errors for the differences between the 48-hour forecasts starting from analysis created by 4D-Var assimilation of cloud radar reflectivity and lidar backscatter observations with doubled observation errors and the operational analysis and between the forecast starting from the reference analysis and the operational analysis. Situation* **2007080100** *with 12-hour assimilation period between 31 July 2007 21:00 UTC and 1 August 2007 09:00 UTC. Reduction (resp. increase) of RMS errors for the experimental run is shown with blue (resp. red) shadings.*

In addition to verifying forecast against model analyses, verification against observations has been also done. Based on 10-day assimilation cycling, forecast departures with respect to TEMP (radiosonde) observations (Fig. 11) indicated an increased skill in predicting tropospheric winds in the experimental run compared to the reference run for the 24 hour forecasts in the Northern hemisphere, where the observations are densest. The skill in 48 hour forecasts is reduced, but still comparable to the reference forecast. Statistics for the tropics and the Southern hemisphere are noisy, suggesting significantly more assimilation cycling is required to draw any significant conclusions. A similar pattern of increased skill in the shorter term forecasts relative to the reference has be seen in radiosonde temperature observations with the greatest improvements in the Southern hemisphere.

Assessment of rain rates in the tropics using independent observations from TRopical Measurement Mission (TRMM) has shown that the RMS in short-term surface rain rate forecasts over the tropics compared to TRMM is reduced by around 2 % when assimilating CloudSat radar reflectivity and CALIPSO lidar backscatter (Fig. 12). The RMS was reduced a further 1 % when using the forecasts initialised with the double error analysis, in agreement with the improved fit to other observation types (e.g., radiosonde) when using double errors.

5 Conclusions

The main objectives of the project was to develop the tools and structure to enable routine EarthCARE radar and lidar observations of clouds to be assimilated in the ECMWF NWP model and to prepare for the real-time monitoring of the observations to detect instrument degradation or errors. This required adjustments of assimilation tools, such as the observation operators, observation error definition, quality control, data screening and bias correction. Several key advances have been made, including a new fast way to account for cloud overlap, increases in operator efficiency and a wholly flow-dependent specification of the observation error.

Based on the in-house automatic monitoring system, data monitoring experiments for cloud radar and lidar observations using CloudSat and CALIPSO data have suggested that the skill of monitoring system to detect a degradation in the quality of observations is improved when the FG departures are used compared to using just observations alone.

The performed assimilation studies have demonstrated the potential which assimilation of cloud information from active sensors could offer. The feasibility to assimilate such observations directly into 4D-Var system in the global scale has been demonstrated for the first time, with improvements in forecast skill shown for temperature and wind. Gaining benefit on forecast skill by including new observations into a well-established observing system is extremely difficult, so the results presented here

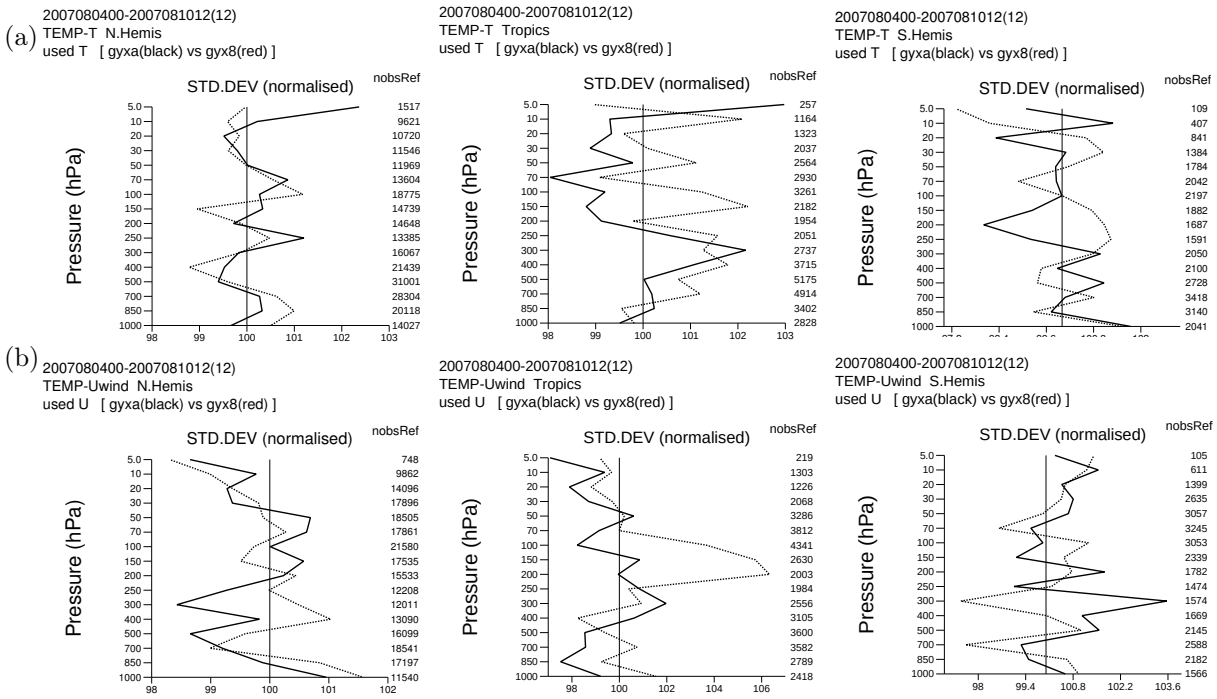

Figure 11: *Normalised standard deviation of forecast departures with respect to TEMP (radiosonde) observations for 24h (solid line) and 48h (dotted line) forecasts for the experiments assimilating cloud radar reflectivity and lidar backscatter using double observation errors and combined with all other routinely assimilated observations. Results are presented for (left) Northern Hemisphere, (middle) Tropics and (right) Southern Hemisphere and for (a) temperature and (b) zonal wind. The number of observations (nobsRef) for the period 4 August 2007 00:00 UTC - 10 August 2007 12:00 UTC is shown at the right side of each profile.*

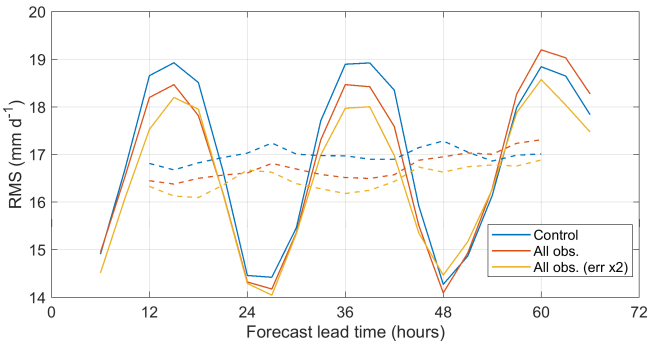

Figure 12: *RMS error between TRMM and forecast near-surface rain rates for varying forecast lead times of up to 3 days. Statistics are generated from forecasts initialised at 00:00 UTC and 12:00 UTC using the reference analysis (***REF***; blue) and all observations analysis (***ALL_RAD_LID***; red). The solid lines indicate a 12 hour averaging window, while the dashed lines indicate a 24 hour averaging window.*

are extremely promising and warrant the opening of many avenues of further research that were not able to be explored here. The sensitivity of the results to the prescribed observation error was shown to be large and it is envisaged that relatively easy gains in forecast skill would be achievable through careful tuning. The behaviour of the assimilation system for different regimes, for example the effect of cloud radar and lidar on convective situations, requires further work and could result in improvements in the forward operator assumptions or screening criteria. No attempt was made to optimise the pre-processing of the observations, so investigations of the averaging scale and possible thinning of the observations in both the horizontal and vertical would be beneficial. Finally, investigation of the synergistic benefit of cloud radar and lidar observations to other observation types related to clouds, in particular the all-sky radiance assimilation framework used at ECMWF, is worthy of further research in the future.

References

Abel, S. J. and I. A. Boutle, 2012: An improved representation of the raindrop size distribution for single-moment microphysics schemes, *Quarterly Journal of the Royal Meteorological Society*, **138**(669), 2151–2162.

Di Michele, S., M. Ahlgrimm, R. Forbes, M. Kulie, R. Bennartz, M. Janisková, and P. Bauer, 2012: Iterpreting and evaluation of the ECMWF global model with CloudSat onbservations: ambiguities due to radar reflectivity forwad operator uncertainties, *Q. J. R. Meteorol. Soc.*, **138**, 2047–2065, doi:10.1002/qj.1936.

ESA, 2004: EarthCARE - Earth Clouds, Aerosol and Radiation Explorer, Reports for mission selection, the sixcandidate Earth explorer missions, ESA SP-1279, ESA Publications Division c/o ESTEC, Noordwijk, The Netherlands.

Illingworth, A. et al., 2015: The earthcare satellite: The next step forward in global measurements of clouds, aerosols, precipitation, and radiation, *Bulletin of the American Meteorological Society*, **96**(8), 1311–1332.

Janisková, M., S. Di Michele, and E. Martins, 2014: Support-to-Science-Elements (STSE) Study - EarthCARE Assimilation, ESA Contract Report on Project 4000102816/11/NL/CT, 225 pp.

Janisková, M., O. Stiller, S. Di Michele, R. Forbes, J.-J. Morcrette, M. Ahlgrimm, P. Bauer, and L. Jones, 2010: QuARL - Quantitative Assessment of the Operational Value of Space-Borne Radar and Lidar Measurements of Cloud and Aerosol Profiles, ESA Contract Report on Project 21613/08/NL/CB, 329 pp.

Kulie, M. S., R. Bennartz, T. J. Greenwald, Y. Chen, and F. Weng, 2010: Uncertainties in microwave properties of frozen precipitation: implications for remote sensing and data assimilation, *J. Atmos. Sci.*, **67**, 3471–3487.

Stephens, G., D. Vane, R. Boain, G. Mace, K. Sassen, Z. Wang, A. Illingwort, E. O'Connor, W. Rossow, and S. Durden, 2002: The CloudSat mission and the A-train, *Bull. Am. Meteorol. Soc.*, **83(12)**, 1771–1790.

Stiller, O., 2010: A flow-dependent estimate for the sampling error, *J. Geophys. Res.*, **115 (D22)**, doi: 10.1029/2010JD013934.

Winker, D., M. Vaughan, A. Omar, Y. Hu, K. Powell, Z. Liu, W. Hunt, and S. Young, 2009: Overview of the CALIPSO mission and CALIOP data processing algorithms, *J. Atmos. and Ocean. Tech.*, **26(7)**, 2310–2323.